Carbohydrate Polymers 90 (2012) 78–86

Contents lists available at SciVerse ScienceDirect

Carbohydrate Polymers

journal homepage: www.elsevier.com/locate/carbpol

Aluminum carboxymethyl cellulose–rice bran microcapsules: Enhancing survival of *Lactobacillus reuteri* KUB-AC5

Pakamon Chitprasert*, Polin Sudsai, Akkaratch Rodklongtan

Department of Biotechnology, Faculty of Agro-Industry, Kasetsart University, Bangkok 10900, Thailand

ARTICLE INFO

Article history:
Received 27 January 2012
Received in revised form 24 April 2012
Accepted 27 April 2012
Available online 6 May 2012

Keywords:
Aluminum carboxymethyl cellulose
Rice bran
Microencapsulation
Survival
Lactobacillus reuteri KUB-AC5

ABSTRACT

This research aimed to enhance the survival of *Lactobacillus reuteri* KUB-AC5 from heat conditioning by using microencapsulation with aluminum carboxymethyl cellulose–rice bran (AlCMC–RB) composites of different weight ratios of 1:0, 1:1, and 1:1.5. The cell/polymer suspension was crosslinked with aluminum chloride at different agitation speeds of 1200, 1500, and 2100 rpm. The AlCMC microcapsules had significantly higher encapsulation efficiency, but lower microcapsule yield than the AlCMC–RB microcapsules ($p \leq 0.05$). Scanning electron microscopy revealed the complexation between AlCMC and RB. Fourier transform infrared spectroscopy showed hydrogen bondings between AlCMC, RB, and cells. The AlCMC–RB microcapsules had significantly lower aluminum ion and moisture contents than the AlCMC ones. After heat exposure, the viability of non-encapsulated and microencapsulated cells in the AlCMC matrix dramatically declined, while that of microencapsulated cells in the AlCMC–RB matrix was about 8 log CFU/g. The results showed the promising potential of the AlCMC–RB composite microcapsules for the protection of probiotics against heat.

1. Introduction

Probiotics are live microorganisms which when administered in adequate amounts confer a health benefit on the host (FAO/WHO, 2002). They have been considered as a potential alternative to antibiotics for animal growth promoters in the post-antibiotic era (Gaggìa, Mattarelli, & Biavati, 2010). One of the selection criteria for potential probiotic strains is heat stability because during pelletizing of animal feeds, high temperature is required (De Angelis et al., 2006). However, most probiotics are heat-sensitive, resulting in a tremendous loss of cell viability during manufacturing processes. This poses a major challenge when using probiotics for industrial applications. Therefore, a heat-protective system for probiotics must be developed for maintaining the cell viability in the range of 1×10^5–1×10^7 CFU/g feed, which is the recommended dosage (Collins, La Ragione, Woodward, & Searle, 2009).

Microencapsulation is an emerging technology for packaging biomolecules or cells in an encapsulation matrix that can provide a desired release characteristic and a physical barrier against adverse environmental conditions (Champagne & Fustier, 2007; de Vos, Faas, Spasojevic, & Sikkema, 2010). One of the widely used techniques for the microencapsulation of probiotics is emulsion-crosslinking. This process is composed of three major steps – the dispersion of cells in encapsulating polymers, emulsification of the cell–polymer suspension in oil, and rigidifying of the polymer hydrogel by crosslinking. The types and concentrations of the encapsulating polymer are considered to be critical factors that affect the efficacy of the microcapsule.

Carbohydrate polymers have received increasingly growing attention as an encapsulating matrix due to their desirable properties such as availability, low cost, non-toxicity, biocompatibility, and biodegradability. The most frequently used carbohydrate polymer for the protection of probiotics against heat is sodium alginate. However, a sodium alginate microcapsule is highly porous in nature, thus allowing the fast diffusion of hot water into the microcapsule (Anal & Singh, 2007; Ding & Shah, 2009; Gouin, 2004). Therefore, a high concentration of sodium alginate up to 4% (w/v) is normally required to improve the heat-protective performance of the microcapsule (Mandal, Puniya, & Singh, 2006; Sabiki, Babu, Thompkinson, & Kapila, 2010).

Sodium carboxymethyl cellulose (NaCMC) is a water-soluble cellulose–ether derivative consisting of β-linked glucopyranose residues with varying levels of carboxymethyl substitution. Application of NaCMC hydrogels has been found in various research fields, including enzyme immobilization (Emregül, Sungur, & Akbulut, 1996) cell cultivation (Chen, Yao, Guan, & Lin, 2005), dye removal (Taleb, Abd El-Mohdy, & Abd El-Rehim, 2009), and drug (Kaihara, Suzuki, & Fujimoto, 2011) and probiotic (Priya, Vijayalakshmi, & Raichur, 2011) delivery. The gastric acid resistance and intestinal solubility properties of NaCMC enable its utilization in drug and probiotic delivery (Kamel, Ali, Jahangir, Shah, & El-Gendy, 2008), while alginate is not a gastro-resistant polymer.

* Corresponding author. Tel.: +66 2 5625085; fax: +66 2 5794096.
E-mail address: pakamon.c@ku.ac.th (P. Chitprasert).

0144-8617/$ – see front matter © 2012 Elsevier Ltd. All rights reserved.
http://dx.doi.org/10.1016/j.carbpol.2012.04.065

However, to our knowledge, there have been no published data on the application of NaCMC microcapsules as heat protectors for probiotics. This could be attributed to its high porosity – a defective characteristic – as found in alginate microcapsules. The high porosity of NaCMC microcapsules is evidenced by their ability to absorb acyclovir, which is an antiviral drug, into the microcapsule (Butun, Ince, Erdugan, & Sahinerdue, 2011). Consequently, the permeability of hot water, whose molecular weight is 12.5 times less than that of acyclovir, must be higher and only low-level cell protection can be obtained.

The present study aimed to develop heat protection microcapsules from NaCMC for increasing the survival of probiotics. The defect of NaCMC microcapsules was reduced by incorporating rice bran (RB) as a filler. Rice bran is obtained as an abundant by-product of rice milling processes. It comprises 14% proteins, 19.8% crude fats, 12.3% acid detergent fibers, 48% carbohydrates, and 6% ash types (Idouraine, Khan, Kohlhepp, & Weber, 1996). It is considered to be a good filler choice because it is commonly used in animal feeds. Moreover, it is a low-cost biomaterial which can help to reduce the production cost of the microcapsule. Changes in the physicochemical properties of the microcapsule by the incorporation of RB were expected to occur due to molecular interactions between the polymer and the filler. This simple structural modification could make the polymer matrix a better heat barrier even at a NaCMC concentration as low as 2% (w/v). *Lactobacillus reuteri* KUB-AC5 was chosen as a model probiotic due to the well-documented research reports of its health benefit for broiler chickens (Nakphaichit et al., 2011). The novel cell-loaded AlCMC–RB composite microcapsule was prepared via the emulsification of the cell–NaCMC suspension with and without RB in palm oil and then crosslinking with aluminum ions. The cell-loaded microcapsules were characterized for the encapsulation efficiency, sizes, size distributions, microcapsule yields, surface morphology, FTIR spectra, aluminum ion contents, and moisture contents. In addition, the cell viability after heat exposure was evaluated to determine an optimum encapsulating condition.

2. Materials and methods

2.1. Materials

NaCMC (high viscosity 700–1500 mPa s, 1% (dry substance) in H_2O at 25 °C, D.S. 0.65–0.90, Fluka), aluminum chloride (Ajax Finechem), sodium chloride (Ajax Finechem), Span 60 (Fluka) and Tween 80 (Ajax Finechem) were of analytical grade. $Na_5P_3O_{10}$ (Sigma–Aldrich) was of practical grade. All chemicals were used as received without any further purification. Palm oil was of food grade (Lam Soon (Thailand) Public Co., Ltd). Rice bran (RB) with a mean particle size of 62.5 μm was sourced from Bangkok, Thailand.

2.2. Methods

2.2.1. Bacterial strain and culture conditions

The microorganism used in this study was *L. reuteri* KUB-AC5 isolated from the small intestine of chicken. The stock cultures were preserved in de Man, Rogosa, and Sharpe (MRS) broth (Merck) containing 20% glycerol at −20 °C. The cells were subcultured in 5 mL MRS broth at 37 °C for 24 h. Then, the cultures were transferred into 30 mL MRS broth at 37 °C for 6 h. The cells were subsequently upscaled using 570 mL MRS broth and incubated under the same condition for 12 h. The cultures were harvested by centrifugation at 4 °C, 8000 rpm for 15 min. The cell pellets were washed twice and resuspended with 0.85% NaCl. The cells were enumerated by a pour-plate method using MRS agar containing 0.6% $CaCO_3$ and by incubating at 37 °C for 48 h.

2.2.2. Preparation of *L. reuteri* KUB-AC5-loaded AlCMC–RB composite microcapsules

Microcapsules of *L. reuteri* KUB-AC5-loaded AlCMC–RB composites were prepared by a typical water-in-oil emulsion external-crosslinking procedure. The external phase was palm oil premixed with 0.025% (w/v) Span 60, while the internal phase was 2.0% (w/v) NaCMC premixed with RB at different weight ratios of 1:0, 1:1 and 1:1.5 (w/w). The mixture of NaCMC and RB was suspended in deionized water using a mechanical overhead stirrer (RW 20n, IKA Laboratory, Germany) with a four-bladed pitched blade turbine and subsequently autoclaved at 110 °C for 10 min. Then, it was mixed with the cell suspension at a ratio of 4:1 (v/v). To obtain the emulsion, the cell/polymer suspension was added dropwise to the oil phase with different agitation speeds of 1200, 1500 and 2100 rpm. A crosslinking agent, 0.05 M $AlCl_3$, was added slowly to harden the microcapsules and break the emulsion. After crosslinking for 2 h, the microcapsules were washed twice for 10 min in 0.3% Tween 80 with an agitation speed of 200 rpm and filtered through Whatman membrane filter No.1. The microcapsules were kept in sterile 0.1% peptone solution at 4 °C until use.

2.2.3. Determination of microencapsulation efficiency

To determine the microencapsulation efficiency of *L. reuteri* KUB-AC5, the microcapsules were dissolved by incubating in 0.04 M $Na_5P_3O_{10}$ at pH 7 for 2 h at 37 °C with horizontal shaking at 250 rpm. The colony forming units (CFU/g) were determined by a pour-plate method using MRS agar containing 0.6% $CaCO_3$ and by incubating at 37 °C for 48 h. Microencapsulation efficiency (ME) was calculated using Eq. (1):

$$\text{ME } (\%) = \frac{N}{N_0} \times 100 \quad (1)$$

where N is the number of microencapsulated cells released from the microcapsules (log CFU/g microcapsule) and N_0 is the number of free cells added to the polymer mixture during the production of the microcapsules (log CFU/g).

2.2.4. Determination of sizes, size distributions, and microcapsule yields

Microcapsule diameters and size distributions were measured using a laser light scattering particle sizer (Mastersizer-2000, Malvern, UK) with wet cell Hydro 2000 MU (A) and 0.05 M $AlCl_3$ as a suspending solution. The volume moment mean diameter ($D[4,3]$) was recorded. Volumes (%) of microcapsules with a size range of 50–500 μm (V) were analyzed with MATLAB Version 7.4 and the microcapsule yield (MY) was then calculated by comparing with the total volume of the microcapsules (V_T) according to Eq. (2):

$$\text{MY } (\%) = \frac{V}{V_T} \times 100 \quad (2)$$

2.2.5. Characterization of surface morphology

A scanning electron microscope (JSM-5600, JEOL, Japan) at an accelerating voltage of 10 kV was used to characterize the external and internal surfaces of the microcapsules prepared under four different microencapsulation conditions of varying NaCMC:RB weight ratios and agitation speeds (rpm), i.e.1:0 and 1200, 1:0 and 2100, 1:1.5 and 1200, and 1:1.5 and 2100, respectively. The beads were incubated in 2% (v/v) osmium tetroxide solution for 1 h, washed twice in distilled water for 10 min each time, and consecutively dehydrated in 30, 50, 70 and 90% (v/v) ethanol solution for 10 min, and in 100% (v/v) ethanol solution three times. Then, they were dried under vacuum using critical point-drying. The microcapsules were fixed on an aluminum stub with double-sided adhesive tape. To expose inner structures, the microcapsules were immersed in

liquid nitrogen and cut with a razor blade, prior to fixation. All samples were sputter-coated with gold using ion sputtering coaters.

2.2.6. Fourier transform infrared spectroscopy (FTIR) studies

FTIR analysis was performed using a TENSOR Series FT-IR spectrometer (Bruker Opics, Germany). The spectra of NaCMC, RB, *L. reuteri* KUB-AC5, and the AlCMC microcapsules prepared with NaCMC:RB ratios of 1:0 and 1:1.5 at 2100 rpm with and without cells were obtained in ATR mode in the 4000–500 cm^{-1} range with a resolution of 4 cm^{-1}.

2.2.7. Determination of aluminum ion contents

The microcapsules were hydrolyzed in concentrated nitric acid and the hydrolysate was analyzed for its aluminum ion contents by flame atomic absorption (AA) spectroscopy (AP300, Shimadzu, Japan). The operating conditions were a nitrous oxide flow rate of 11 L/min, an acetylene flow rate of 7 L/min, lamp current of 10 mA, wavelength of 309.3 nm and spectral bandpass of 0.7 nm.

2.2.8. Determination of moisture contents

The moisture contents of the microcapsules were determined gravimetrically, based on a difference in the weight before and after drying in a hot air oven at 103 ± 2 °C for 48 h.

2.2.9. Determination of cell survival after heat exposure

A heat test was carried out by incubating 1 g of free and microencapsulated cells in a test tube containing 49 mL of sterile distilled water at 85 °C for 25 s and immediately immersing in chilled water to room temperature within 3 min. The enumeration of viable cells was performed as described previously in Section 2.2.3. The percentage of cell survival was calculated according to Eq. (3):

$$\text{Cell survival}\,(\%) = \frac{N_F}{N_I} \times 100 \tag{3}$$

where N_I and N_F is the number of viable microencapsulated cells released from the microcapsules before and after the heat test (log CFU/g microcapsule), respectively.

2.2.10. Statistical analysis

A full factorial design for two factors at three levels consisting of nine combinations was used for the experiment. All experiments were performed in triplicate. Statistical analysis was undertaken using one-way ANOVA. The data were presented as mean values ± standard deviation (SD). The statistical significance of the results was evaluated using Duncan's multiple range test (DMRT) at the 95% confidence level.

3. Results and discussion

In this present research, microencapsulated *L. reuteri* KUB-AC5, an effective probiotic for broiler chicken, was prepared by forming a water-in-oil emulsion, followed by droplet gelation via ionic crosslinking. To optimize the microencapsulation conditions, two parameters, i.e. NaCMC:RB ratios and agitation speeds, were evaluated. The cells were initially suspended in the autoclaved mixture of NaCMC and RB with three different weight ratios of 1:0, 1:1 and 1:1.5 and were subsequently emulsified in palm oil containing Span 60 at different turbine agitation speeds of 1200, 1500 and 2100 rpm. By adding aluminum chloride, the aqueous polymer/cell-containing droplets gradually underwent external gelation (hardening) of the polymers. Since the pH of the polymer/cell suspension was 6.3 which was above the pKa of carboxylic groups of NaCMC (approximately pH 4.3), the carboxylic groups became ionized and interacted electrostatically with the aluminum ions. The physical crosslinking resulted in the partial expulsion of water trapped between the NaCMC chains together with the formation of a three-dimensional structure entrapping the cells. The characteristics of the water-insoluble microcapsules influencing the ability to protect the cells against moist heat and cell survival after heat exposure were analyzed.

3.1. Microencapsulation efficiency

The first characteristic of the microcapsules investigated here was microencapsulation efficiency indicating the cell viability during the microencapsulation process combined with the cell retainability. It is desirable that the number of live cells entrapped in the microcapsules is high in order to potentially increase the number of cells remaining after being subjected to heat. The results in Table 1 reveal that there was only a small loss of cell viability and high cell retainability during the microcapsule preparation. From the initial cell number of 11.14 log CFU/g, a microencapsulation efficiency of approximately 99% (11.03 log CFU/g microcapsule) was achieved with a NaCMC:RB ratio of 1:0, irrespective of the agitation speed. The high microencapsulation efficiency can be attributed to four reasons. First, NaCMC appears to be a suitable encapsulating polymer for *L. reuteri* KUB-AC5 due to its nontoxicity. It was found that when chitosan was used as the encapsulating material, it provided only 78% microencapsulation efficiency as a result of toxicity on Gram-positive *L. reuteri* KUB-AC5 (data not shown). Second, mixing the bacteria with NaCMC using a mechanical overhead stirrer with a four-bladed pitched blade turbine at a high speed of up to 2100 rpm appears to be a gentle method. Our results are in agreement with those reported by Capela, Hay, and Shah (2007) and Ding and Shah (2009) that unlike a homogenizer, a stirrer as a simple device applied in the traditional standard emulsion technique does not mechanically cause cell rupture from impact, shear, and heat stress, thereby providing high survival of the bacteria. Third, during the formation of the water-insoluble gel structures, the polymer shell allows only water molecules to diffuse out of the microcapsules into the surrounding fluid, whereas the bacterial cells that are considerably larger in size (0.8 μm × 1.6 μm) remain trapped inside. Fourth, there is no noticeable loss of cells from the microcapsules during the washing step for oil removal with a low agitation speed of 200 rpm. With the same emulsion-crosslinking technique, the microencapsulation efficiency of the AlCMC microcapsules with RB was still high, but significantly decreased ($p \leq 0.05$). From the initial cell number of 11.68 log CFU/g, the encapsulated cell number was reduced to 10.63 log CFU/g microcapsule (91% microencapsulation efficiency) suggesting that the incorporation of RB, containing a high content of insoluble dietary fiber of up to 23.6% (Idouraine et al., 1996), whose structure is densely packed, might partly block the cell entrapment.

3.2. Sizes, size distributions, and microcapsule yields

The size of probiotic-loaded microcapsules is an important characteristic of feed additives in poultry production. To ensure a satisfactory mixing ability that can directly influence the adequate homogeneity of feed additives and the correct dosage for animals, a feed additive size range of 50–500 μm is recommended. Therefore, this size range was used as the criterion to determine the microcapsule yield and the optimal microencapsulation condition. As shown in Table 1, NaCMC:RB ratios of 1:1 and 1:1.5 at an agitation speed of 2100 rpm were found to be the optimal microencapsulation conditions providing the greatest microcapsule yields of approximately 99%. Conversely, microencapsulation with a NaCMC:RB ratio of 1:0 provided lower microcapsule yields, particularly at an agitation speed of 1200 rpm. The volume moment mean diameters ($D[4,3]$) of the microcapsules prepared under different conditions ranged from 159.92 to 661.19 μm. As the agitation

Table 1
Microencapsulation efficiency, microcapsule yields and the volume moment mean diameters (D[4,3]) of *L. reuteri* KUB-AC5-loaded AlCMC–RB microcapsules prepared under different conditions.

NaCMC:RB ratio	Agitation speed (rpm)	Microencapsulation efficiency (%)	Microcapsule yield (%)	D[4,3] (μm)
1:0	1200	99.26 ± 0.90^{a}	25.73 ± 0.06^{f}	661.19 ± 11.93^{i}
	1500	99.71 ± 0.33^{a}	40.71 ± 0.97^{e}	544.99 ± 9.63^{h}
	2100	99.11 ± 0.58^{a}	77.08 ± 0.61^{c}	346.63 ± 5.59^{f}
1:1	1200	91.45 ± 0.25^{bcd}	56.64 ± 2.19^{d}	403.26 ± 10.22^{g}
	1500	90.84 ± 0.38^{de}	79.85 ± 2.49^{c}	289.05 ± 11.06^{e}
	2100	91.69 ± 0.38^{bc}	99.25 ± 0.24^{a}	178.09 ± 7.50^{b}
1:1.5	1200	90.57 ± 0.11^{e}	80.88 ± 2.06^{c}	269.21 ± 8.95^{d}
	1500	90.93 ± 0.54^{cde}	86.00 ± 6.31^{b}	231.77 ± 9.52^{c}
	2100	91.78 ± 0.03^{b}	98.51 ± 0.84^{a}	159.92 ± 3.96^{a}

[a–h]Means ± standard deviation with different superscript letters in the same column indicate significant differences ($P < 0.05$) between the microcapsules.

speed increased at a given NaCMC:RB ratio, the average microcapsule diameters decreased significantly. This was possibly due to an increase in the turbulent flow causing more effective dispersion of aqueous droplets of the cell-loaded polymer in the oil phase during emulsification which is the critical step defining the microcapsule size. This result was in accordance with that of Brown, Kessler, Sottos, and White (2003) who showed that it was possible to obtain a fine oil-in-water emulsion that later turned into a small microcapsule of poly(urea–formaldehyde) loaded with dicyclopentadiene by using the high agitation speed of a propeller. Moebus, Siepmann, and Bodmeier (2009) also published a similar finding that an increase in the propeller speed resulted in a small-sized drug-loaded alginate-poloxamer microparticle.

Table 1 also reveals that not only an increase in the agitation speed, but also that an increase in the RB amounts led to a noticeable decrease in the microcapsule size. This could be attributed to the excellent lipophilic emulsifying property of an oil-soluble fraction of RB (Yun & Hong, 2007) that can additionally reduce the interfacial tension of aqueous droplets in contact with oil besides Span 60, an intentionally added emulsifier. Moreover, after autoclaving, RB partially dissolved and became smaller in size. They could adsorb Span 60 and thereby additionally lower the interfacial tension.

The pronounced effect of the RB amount and agitation speed on the particle size distribution of the *L. reuteri* KUB-AC5-loaded microcapsules is shown in Fig. 1. With increasing RB amounts and agitation speeds, the particle size distribution appeared to be more positively skewed and have a more distinct bimodal size distribution. Regarding the microcapsule size, the optimal preparation conditions of the microcapsules are NaCMC:RB ratios of 1:1 and 1:1.5 at an agitation speed of 2100 rpm.

3.3. Surface morphology

Scanning electron microscopy (SEM) was used to characterize the internal and external surface morphology of the *L. reuteri* KUB-AC5-loaded microcapsules prepared under four different microencapsulation conditions of NaCMC:RB ratios and agitation speeds, i.e.1:0 and 1200 rpm; 1:0 and 2100 rpm; 1:1.5 and 1200 rpm; 1:1.5 and 2100 rpm, respectively. As displayed in Fig. 2a, most of the microcapsules without RB at 1200 rpm were agglomerated into non-spherical clusters, which resulted in large sizes, and were relatively highly polydispersed. However, the microcapsules became more nearly spherical in shape and individually dispersed with high agitation speeds and the presence of RB (Fig. 2b–d). Microscopic cracks and wrinkles as a result of the partial collapse of the polymer network along with the loss of water during sample preparation for SEM were more visibly observed on the external surfaces of the AlCMC samples (Fig. 2e and f) than on the AlCMC–RB samples (Fig. 2g and h). Dense populations of short rod-shaped bacteria were also observed bulging on the external surfaces of all samples, which were similar to the external surface morphology of calcium-alginate microcapsules loaded with *Bifidobacterium* spp. prepared by the same method (Truelstrup Hansen, Allan-Wojtas, Jin, & Paulson, 2002). The interior of the fractured microcapsules revealed that a great number of the cells were distributed randomly within the polymer matrices (Fig. 2i–l). At higher magnification, SEM further showed that the AlCMC

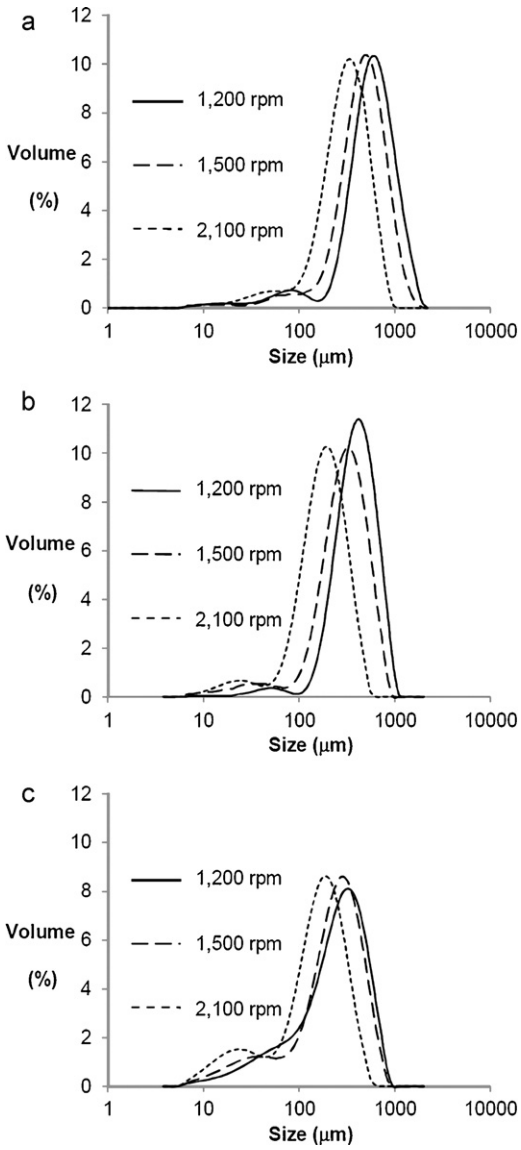

Fig. 1. Size distributions of *L. reuteri* KUB-AC5-loaded AlCMC–RB microcapsules prepared with different agitation speeds and NaCMC:RB ratios: (a) 1:0, (b) 1:1, and (c) 1:1.5.

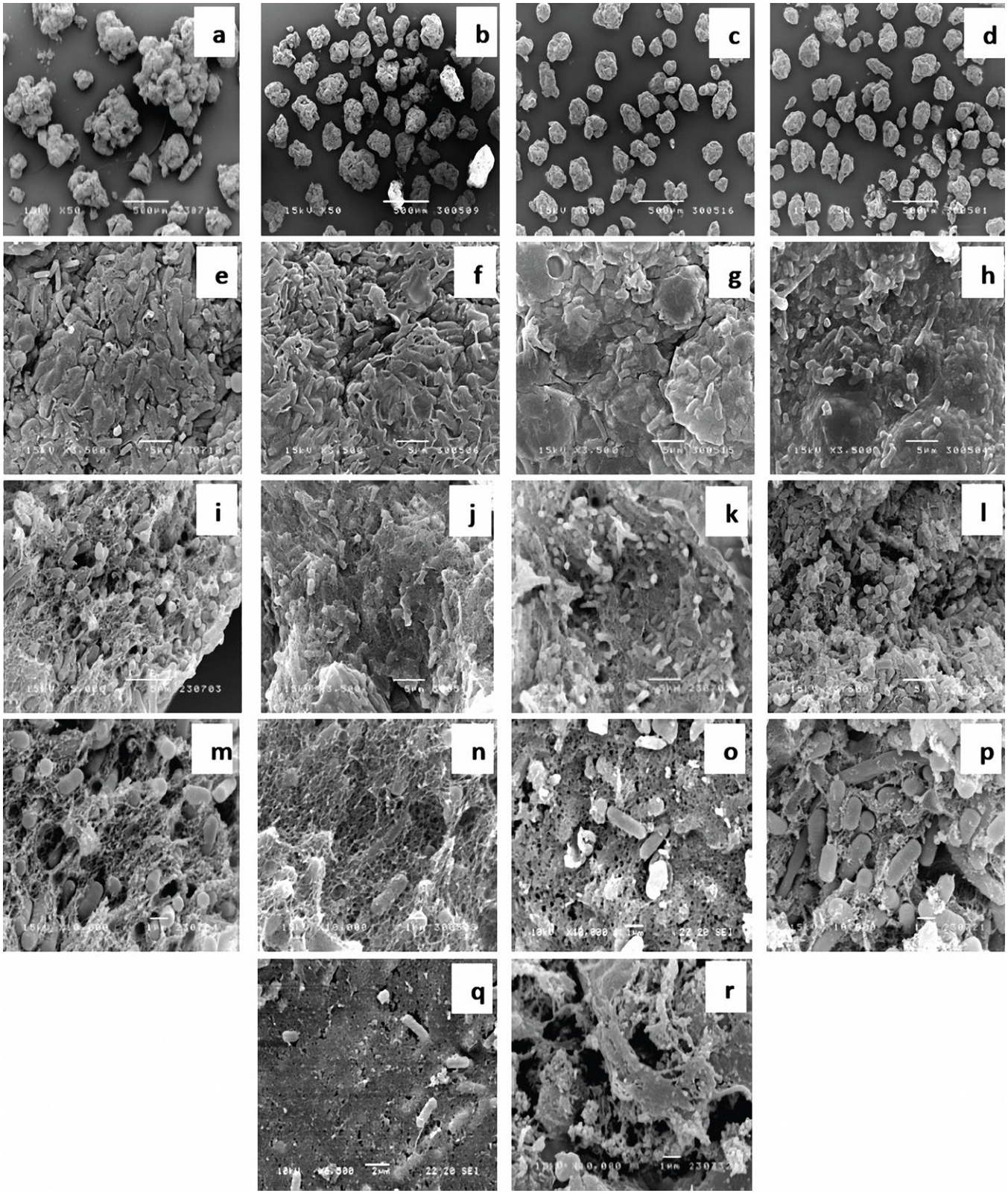

Fig. 2. SEM of whole and fractured AlCMC and AlCMC–RB microcapsules loaded with *L. reuteri* KUB-AC5, and RB. Whole microcapsules prepared from NaCMC:RB (1:0) with 1200 and 2100 rpm (a and b, respectively). Whole microcapsules prepared from NaCMC:RB (1:1.5) with 1200 and 2100 rpm (c and d, respectively). Outer surface areas of microcapsules prepared from NaCMC:RB (1:0) with 1200 and 2100 rpm (e and f, respectively). Outer surface areas of microcapsules prepared from NaCMC:RB (1:1.5) with 1200 and 2100 rpm (g and h, respectively). Inner surface areas of microcapsules prepared from NaCMC:RB (1:0) with 1200 and 2100 rpm (i and j, respectively). Inner surface areas of microcapsules prepared from NaCMC:RB (1:1.5) with 1200 and 2100 rpm (k and l, respectively). Higher magnification view of inner surface areas of microcapsules prepared from NaCMC:RB (1:0) with 1200 and 2100 rpm (m and n, respectively). Higher magnification view of inner surface areas of microcapsules prepared from NaCMC:RB (1:1.5) with 1200 and 2100 rpm (o and p, respectively). Dense matrices of microcapsules prepared from NaCMC:RB (1:1.5) with 2100 rpm. RB morphology (r).

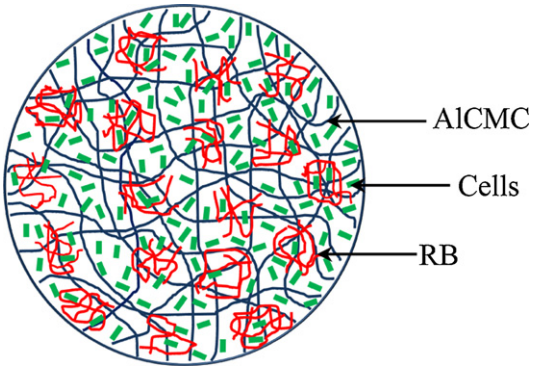

Fig. 3. Schematic diagram of *L. reuteri* KUB-AC5-loaded AlCMC–RB microcapsules.

matrices (Fig. 2m and n) had a homogeneous mesh-like topology over the entire network. The structural homogeneity of the AlCMC matrices might stem from the slow gelation rate due to the slow addition of aluminum chloride (7.4 mL/min) and the effective crosslinking due to the low viscosity of NaCMC (Kuo & Ma, 2001). The high-magnification SEM images also showed that the porous AlCMC matrices surrounding the cells were similar in structure to the matrix interiors of the microcapsules. In contrast with our observations, Allan-Wojtas, Truelstrup Hansen, and Paulson (2008) reported that *Bifidobacterium lactis* Bb-12 encapsulated in calcium-alginate microcapsules was instead surrounded by a smooth layer of calcium-alginate similar to the exterior surfaces. The interiors of the AlCMC–RB microcapsules (Fig. 2o and p) were dense matrices and in some regions (Fig. 2q), the cells were hardly observed, which corresponded with a low microencapsulation efficiency. The dense matrices of the AlCMC–RB microcapsules were composed of dense RB sheets and AlCMC-entrapped RB interstices (Fig. 2r). For a better understanding of the structure of the AlCMC–RB microcapsules loaded with cells, a schematic diagram is provided in Fig. 3.

Since the ability to protect the cells against heat is a desirable characteristic of the microcapsules, the dense matrices are required to effectively prevent the penetration of hot water. Considering the SEM images of all the microcapsules presented here, the AlCMC microcapsules with RB should provide more superior heat barrier properties than those without RB. However, to confirm this postulation, a heat test was carried out in a later section.

3.4. FTIR characterization

FTIR was employed to explore the structural information of NaCMC, RB, *L. reuteri* KUB-AC5, and their interactions in the presence of aluminum ions as crosslinking agents. The first group of FTIR spectra shown in Fig. 4 a belongs to NaCMC, RB, as well as AlCMC:RB (1:0) and AlCMC:RB (1:1.5) microcapsules without cells. In the case of the NaCMC spectum, the broad band at 3339 cm^{-1} represented the O—H stretching vibrations. The asymmetric and symmetric stretching vibrations of aliphatic C—H were observed at 2922 and 2853 cm^{-1}, respectively, while those of C(=O)—O$^-$ were observed at 1581 and 1413 cm^{-1}, respectively. The peak at 1323 cm^{-1} was assigned to the C—O stretching vibrations. The very weak peak at 1204 cm^{-1} belonged to the O—H bending vibrations, while the C—O—C (glycosidic linkage) stretching vibrations were indicated by the peaks at 1053, 1022, and 897 cm^{-1}. Due to the ionic crosslinking, NaCMC solution underwent a gelation process to form AlCMC microcapsules, which was confirmed by the increase in intensity of intermolecular hydrogen bonds among the hydroxyl groups. In addition, the crosslinked spectra showed shifts of the O—H stretching vibrations by −4 cm^{-1}, O—H bending vibrations by +35 cm^{-1} as well as asymmetric and symmetric C(=O)—O$^-$ stretching vibrations by +58 and +52 cm^{-1}, respectively. The intensities of

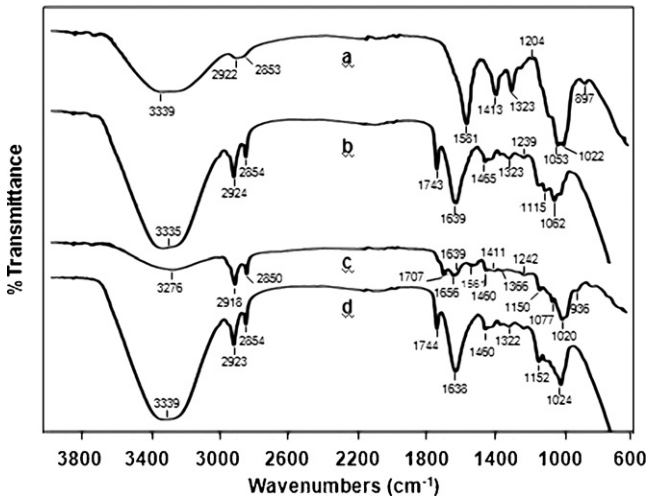

Fig. 4. FTIR spectrum of (a) NaCMC, (b) microcapsules prepared from NaCMC:RB (1:0), (c) RB, and (d) microcapsules prepared from NaCMC:RB (1:1.5).

these C(=O)—O$^-$ peaks were also lessened. The shift of the C—O—C stretching vibrations to higher wave numbers along with a reduction in their intensities was observed. The transformation of NaCMC solution to AlCMC hydrogel was also reflected by the appearance of the new peak at 1743 cm^{-1} denoting the C=O stretching vibrations and the disappearance of the peak at 897 cm^{-1}.

For the RB spectrum, the fatty acid region was in the range of 3300–1700 cm^{-1}. The band at 3276 cm^{-1} represented the O—H stretching vibrations, which overlapped the N—H stretching vibrations in the same region. The asymmetric and symmetric aliphatic C—H stretching vibrations were indicated by the peaks at 2918 and 2850 cm^{-1}, respectively. The band at 1707 cm^{-1} was due to the C=O stretching vibrations of ester functional groups primarily from fatty acids. The amide region of the proteins was in the range 1700–1500 cm^{-1}. The bands at 1656 and 1639 cm^{-1} indicated the stretching vibrations of C=O (amide I) and asymmetric stretching vibrations of C(=O)—O$^-$. The bands between 1561 and 1500 cm^{-1} were assigned to the N—H bending vibrations of amide II. The mixed region of RB proteins and fatty acids was in the range 1500–1200 cm^{-1}. The very weak peak at 1460 cm^{-1} represented C—H bending vibrations. A symmetric stretching vibration of C(=O)—O$^-$ was observed at 1411 cm^{-1}. The very weak peak at 1366 cm^{-1} indicated the C—O stretching vibrations. The peak at 1242 cm^{-1} represented the C—N stretching vibrations. The bands at 1150, 1077, 1020, and 936 cm^{-1} denoted the C—O—C stretching vibrations of polysaccharides.

During the formation of the AlCMC:RB (1:1.5) microcapsules, the interaction between RB, NaCMC, and aluminum ions was evidenced by the abrupt shift of the O—H and N—H stretching vibrations of RB to a higher wavenumber by +63 cm^{-1} with a higher intensity. The peak of the C=O stretching vibrations at 1656 and 1639 cm^{-1} in the RB spectrum turned into the broad peak at 1638 cm^{-1} in the microcapsule spectrum and the weak bands between 1561 and 1500 cm^{-1} disappeared. This indicated that the O—H, N—H, and C=O of RB were involved in the interaction. Meanwhile, the conformational change of NaCMC after crosslinking with aluminum ions and forming composite microcapsules with RB was shown by the appearance of the new peak at 1744 cm^{-1} denoting the C=O stretching vibrations in the spectrum of composites. The location of this band was very close to 1743 cm^{-1} in the AlCMC microcapsule spectrum. The involvement of C(=O)—O$^-$ of NaCMC in such an interaction was shown by the significant shift of its asymmetric and symmetric stretching vibrations to higher wavenumbers by +57 and +47 cm^{-1}, respectively. A shift

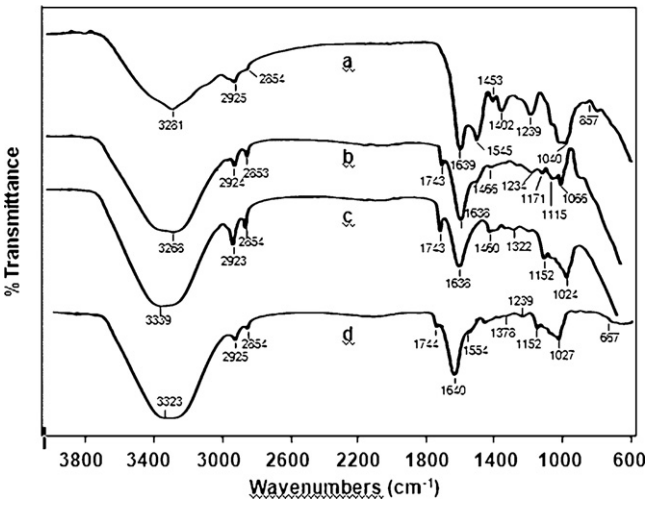

Fig. 5. FTIR spectra of (a) *L. reuteri* KUB-AC5, (b) cell-loaded microcapsules prepared from NaCMC:RB (1:0), (c) microcapsules prepared from NaCMC:RB (1:1.5), and (d)) cell-loaded microcapsules prepared from NaCMC:RB.

by +38 cm^{-1} of the O—H bending in the NaCMC spectrum was also found. As previously observed in the structural change of NaCMC to AlCMC without the complexation with RB, the shift of the C—O—C stretching vibrations to higher wave numbers along with a reduction in the intensity occurred. Thus, it is likely that RB does not obviously interfere with the crosslinking between NaCMC and the aluminum ion during the microcapsule formation. The rest of the bands in the NaCMC and RB spectra retained their positions after the composite formation and crosslinking.

The second group of FTIR spectra shown in Fig. 5 belongs to *L. reuteri* KUB-AC5, the AlCMC:RB (1:0) microcapsules loaded with cells, as well as the AlCMC:RB (1:1.5) microcapsules with and without cells. The FTIR spectrum of the cells identifies the characteristics of cell components including fatty acids, proteins, polysaccharides, and nucleic acids. The bands representing the asymmetric stretching vibrations of CH_3 and CH_2, typical functional groups present in fatty acids as cell membrane components, were located at 2925 and 2854 cm^{-1}, respectively (Kansiz et al., 1999; Kummerle, Schererm, & Seiler, 1998). The proteins were indicated by the peaks of the C═O stretching vibrations of amide I at 1639 cm^{-1} (Choo-Smith et al., 2001), the N—H bending vibrations of amide II at 1545 cm^{-1}, as well as the CH_3 and CH_2 asymmetric and symmetric bending vibrations at 1453 and 1402 cm^{-1} (Filip & Hermann, 2001). The region of 1300–900 cm^{-1} was referred as the fingerprint region representing the spectral characteristics of cell components (Goodacre, Timmins, Rooney, Rowland, & Kell, 1996). The P═O asymmetric and symmetric stretching vibrations of the phosphodiester backbone of nucleic acids were located at 1239 and 857 cm^{-1}, respectively, and the C—O—C stretching vibrations of polysaccharides as the components of cell wall glycopeptides and lipopolysaccharides were also observed in the same region (Choo-Smith et al., 2001; Filip & Hermann, 2001; Kansiz et al., 1999).

The interaction between the cells, NaCMC, and aluminum ions during the formation of the cell-loaded microcapsules was also investigated by FTIR. The location of the band assigned to the O—H and N—H stretching vibrations of the cells was lower by −13 cm^{-1}. The peak denoting the N—H bending vibrations vanished in the spectrum of the AlCMC microcapsules loaded with cells. The peaks of the CH_3 and CH_2 asymmetric and symmetric bending vibrations appearing as a doublet at 1453 and 1402 cm^{-1} in the cell spectrum moved to a higher level at 1466 cm^{-1}. All the cell spectral peaks in the region below 1402 cm^{-1} indicated that the P═O and C—O—C stretching vibrations were still present. When NaCMC was mixed with the cells in the presence of aluminum ions, its spectral change was similar to that when mixed with RB and the crosslinking reaction still occurred.

The spectrum of the AlCMC:RB (1:1.5) microcapsules loaded with cells contained all the peaks found for both the AlCMC microcapsules loaded with cells and the AlCMC:RB (1:1.5) microcapsules without cells. It was clearly observed that among these three samples, the AlCMC:RB (1:1.5) microcapsules loaded with cells displayed the strongest and broadest peak at 3323 cm^{-1} representing the O—H and N—H stretching vibrations, which might be a result from the intermolecular hydrogen bondings between the components. Hence, the cells strengthened the interaction between AlCMC and RB.

Table 2
Aluminum ions and moisture contents of *L. reuteri* KUB-AC5-loaded AlCMC–RB microcapsules prepared under different conditions.

NaCMC:RB ratio	Agitation speed (rpm)	Aluminum ion contents (mg/g microcapsule)	Moisture content(%)
1:0	1200	30.96 ± 0.10	82.29 ± 1.32^{e}
	1500	27.00 ± 0.23^{b}	78.12 ± 0.96^{d}
	2100	20.88 ± 0.08^{c}	72.48 ± 0.73^{c}
1:1	1200	0.14 ± 0.07^{f}	73.70 ± 0.50^{c}
	1500	0.34 ± 0.09^{e}	72.71 ± 0.45^{c}
	2100	0.48 ± 0.02^{de}	72.53 ± 0.22^{c}
1:1.5	1200	0.35 ± 0.06^{e}	73.69 ± 0.07^{c}
	1500	0.44 ± 0.05^{de}	71.21 ± 0.29^{b}
	2100	0.61 ± 0.06^{d}	66.24 ± 0.33^{a}

$^{a-f}$ Means ± standard deviation with different superscript letters in the same column indicate significant differences ($P < 0.05$) between the microcapsules.

3.5. Aluminum ion contents

AA was used to measure the total amount of aluminum ions, which can be either electrostatically crosslinked or unbound to available free negative ions, especially the carboxylate ions of NaCMC constituting the microcapsules. As shown in Table 2, all of the microcapsules with RB had significantly less aluminum ion contents than those without RB ($p \leq 0.05$), although the crosslinking condition including the concentration of aluminum chloride and the crosslinking time applied for each treatment was the same. The overall result apparently indicates that due to the structural components of the AlCMC–RB composites composed of the dense RB sheets and the tortuous AlCMC-entrapped RB interstices, they effectively hinder the inward convective transport of aluminum ions during the crosslinking reaction. Similarly, Vale, Justice, Schaefer, and Mark (2007) found that by impregnating calcium–alginate films with 0.5% dried weight Montmorillonite clay to increase the diffusion path length, the permeation of benzaldehyde was decreased by approximately 2.5 times compared to nascent films. It can also be observed from Table 2 that the AlCMC:RB microcapsules (both 1:1 and 1:1.5) prepared at 2100 rpm had significantly higher aluminum ion contents than those prepared at 1200 rpm ($p \leq 0.05$). A possible explanation for this phenomenon is that the AlCMC:RB microcapsules prepared at 2100 rpm have a smaller droplet size as a result of the higher agitation speed; therefore, they have a larger specific surface area which is beneficial to the absorption of aluminum ions. Even though very small amounts of aluminum ions were detected in the AlCMC microcapsules with RB, based on the stoichiometric ratio, they were present in an excess amount for the crosslinking reaction. Moreover, RB contains metals available in the form of di- and trivalent cations such as iron, magnesium, calcium, and copper ions (Montanher, Oliveira, & Rollemberg, 2005), all of which can participate in the reaction with the carboxylate ions of NaCMC to promote the three-dimensional crosslinked network.

Table 3
Survival of non-microencapsulated and encapsulated *L. reuteri* KUB-AC5 prepared under different conditions after 25 s exposure at 85 °C.

NaCMC:RB ratio	Agitation speed (rpm)	Initial cells (log CFU/g microcapsule)	Final cells (log CFU/g microcapsule)	Cell survival (%)
Free cells	–	11.29 ± 0.04	4.76 ± 0.14	42.17 ± 1.26[h]
Microencapsulated cells				
	1200	11.00 ± 0.54	5.41 ± 0.24	49.16 ± 0.64[g]
1:0	1500	11.03 ± 0.44	5.62 ± 0.26	51.05 ± 0.15[f]
	2100	10.51 ± 0.26	6.14 ± 0.37	55.86 ± 1.75[e]
	1200	10.81 ± 0.04	7.56 ± 0.04	69.93 ± 0.56[d]
1:1	1500	10.69 ± 0.02	7.74 ± 0.04	72.41 ± 0.53[c]
	2100	10.81 ± 0.08	8.07 ± 0.08	74.71 ± 0.9[ab]
	1200	10.63 ± 0.03	7.71 ± 0.07	72.51 ± 0.62[c]
1:1.5	1500	10.68 ± 0.06	7.88 ± 0.03	73.77 ± 0.61[bc]
	2100	10.75 ± 0.06	8.11 ± 0.02	75.46 ± 0.22[a]

[a-h] Means ± standard deviation with different superscript letters in the same column indicate significant differences ($P < 0.05$) between the microcapsules.

3.6. Moisture contents

The moisture contents of the cell-loaded microcapsules presented in Table 2 exhibit a somewhat similar trend to the aluminum ion contents. The lowest and highest moisture contents were achieved with NaCMC:RB ratios of 1:1.5 at 2100 rpm and 1:0 at 1200 rpm, respectively. The moisture contents in the treatment group of NaCMC:RB (1:1.5) were generally lower than those in other treatments. This implies that the water-holding capacity of RB is lower than that of NaCMC even though RB contains large amounts of insoluble fiber possessing tremendous water-holding capacity (Hu, Huang, Cao, & Ma, 2009). It also appears that the moisture contents in the treatment group of NaCMC:RB (1:1.5) decreased with increasing agitation speeds. This can be explained by the fact that at high agitation speeds, the interstitial spaces (where water is located) between the NaCMC chains are reduced. In other words, high agitation speeds result in effective water expulsion during the transformation of the polymer droplets to the microcapsules. The impact of agitation speed on lowering the moisture content was also detected in the control group of NaCMC:RB (1:0), which had a relatively high moisture content compared to the other groups. Due to the large amount of water present in the NaCMC droplets without RB, inlet flow of aluminum ions through the droplets was not prevented as shown by the results in the previous section. Regarding moisture content, the microcapsules obtained from the conditions of NaCMC:RB (1:1.5) and 2100 rpm should have had the highest density, which is beneficial to enhance the heat barrier property of the microcapsule.

3.7. Survival of L. reuteri KUB-AC5 after heat exposure

To investigate the efficacy of the microcapsules in protecting *L. reuteri* KUB-AC5 against heat, the survival of microencapsulated cells and free (non-microencapsulated) cells as controls was evaluated after exposure to a lethal heat stress of 85 °C for 25 s, a condition required to prepare pelleted broiler feeds. The cell viability from statistical analysis in Table 3 could be ranked from the free cells < microencapsulated cells in AlCMC matrices < microencapsulated cells in AlCMC–RB matrices ($p \leq 0.05$) and it increased with increasing agitation speeds at a constant NaCMC:RB ratio. The number of free cells was substantially reduced (more than 57%) due to heat shock, although *L. reuteri* KUB-AC5 was reported to be a thermotolerant bacterium (Nitisinprasert et al., 2000). Because of the heat protection provided by the polymer matrices, all of the microencapsulated cells had significantly higher survival rates than the free cells, but the ones in the AlCMC matrices had survival only up to ~6 log CFU/g microcapsule. The reason that the AlCMC microcapsules offered little heat protection could be due to the fact that the microcapsules have high free volume arising from the low concentration of CMC at 2% (w/v), which promoted the permeability of hot water. However, an increase in the agitation speed enhanced the protective effect of the AlCMC microcapsules because high agitation speeds can decrease the free volume of the polymer, which simultaneously results in dense and small diameter microcapsules. Even though the small diameter of the microcapsule facilitates the fast radial mass transfer of hot water, its high density alleviates this negative effect.

The cells in the AlCMC–RB (both 1:1 and 1:1.5) microcapsules were detected in rather high counts up to 8 log CFU/g microcapsule. The highest cell survival (~75%) was obtained with the ones prepared at 2100 rpm. As mentioned above, the presence of RB together with a high agitation speed increased the diffusion path length and density, which are beneficial in reducing the amount of hot water passing through the microcapsule. Only the cells on the external surface have an extensive loss of viability due to their direct contact with hot water. Previous studies have shown that the high-density structure of the encapsulating matrix was necessary to enhance the survival rate of probiotic bacteria. However, high gel concentrations were used to obtain the dense matrix. For example, Mandal et al. (2006) reported that the highest survival of *Lactobacillus casei* NCDC-298 after incubation in hot water at 65 °C for 20 min was recorded in 4% calcium-alginate beads, followed by 3%, and 2%. The minimum concentration of 3% calcium-alginate beads was always required if calcium-alginate was used as the only encapsulating material for the heat protection of probiotics (Ding & Shah, 2007). Another approach that has been successfully used to form heat protective microcapsules is to combine alginate with other biomaterials. For instance, Sabiki et al. (2010) found that the *Lactobacillus acidophilus* LA1 encapsulated with 4% calcium alginate and 2% native corn starch was reduced by 4.14 log cycles after being subjected to heat treatment at 90 °C for 30 s, whereas the free cells were completely destroyed (~9.13 log cycle reduction). Chen, Chen, & Kuo (2007) reported that under heat treatment in hot water at 75 °C for 1 min, *Bifidobacterium bifidum* encapsulated in 0.50, 1.25, or 2.00% alginate mixed with 0.50, 0.75, or 1.00% gellan had the highest survival with the highest concentration of each polymer.

4. Conclusions

The heat survival of a model probiotic, *L. reuteri* KUB-AC5, was successfully enhanced by microencapsulating with AlCMC–RB composites. The microencapsulation condition of NaCMC:RB ratios of 1:1 and 1:1.5 adversely affected the microencapsulation efficiency, but positively affected the yield and density. The viable cell number of free cells and microencapsulated cells in the AlCMC microcapsules after heat exposure was not enough to exert a

beneficial health effect to animals, while that of microencapsulated cells in the AlCMC–RB composite microcapsules, particularly prepared at 2100 rpm was about 8 log CFU/g microcapsule. The knowledge obtained from this research can fruitfully be applied to the development of probiotic products as functional feeds that require heat treatment.

Acknowledgment

This work was financially supported by the Kasetsart University Research and Development Institute (KURDI) under grant No. SRU-11.49.

References

Abou Taleb, M. F., Abd El-Mohd, H. L., & Abd El-Rehim, H. A. (2009). Radiation preparation of PVA/CMC copolymers and their application in removal of dyes. *Journal of Hazardous Materials*, *168*, 68–75.

Allan-Wojtas, P., Truelstrup Hansen, L., & Paulson, A. T. (2008). Microstructural studies of probiotic bacteria-loaded alginate microcapsules using standard electron microscopy techniques and anhydrous fixation. *Lebensmittel-Wissenschaft und-Technologie*, *41*, 101–108.

Anal, A. K., & Singh, H. (2007). Recent advances in microencapsulation of probiotics for industrial applications and targeted delivery. *Trends in Food Science and Technology*, *18*, 240–251.

Brown, E. N., Kessler, M. R., Sottos, N. R., & White, S. R. (2003). In situ poly(urea-formaldehyde) microencapsulation of dicyclopentadiene. *Journal of Microencapsulation*, *20*, 719–730.

Butun, S., Ince, F. G., Erdugan, H., & Sahiner, N. (2011). One-step fabrication of biocompatible carboxymethyl cellulose polymeric particles for drug delivery systems. *Carbohydrate Polymers*, *86*, 636–643.

Capela, P., Hay, T. K. C., & Shah, N. P. (2007). Effect of homogenisation on bead size and survival of encapsulated probiotic bacteria. *Food Research International*, *40*, 1261–1269.

Champagne, C. P., & Fustier, P. (2007). Microencapsulation for the improved delivery of bioactive compounds into foods. *Current Opinion in Biotechnology*, *18*, 184–190.

Chen, M., Chen, K., & Kuo, Y. (2007). Optimal thermotolerance of *Bifidobacterium bifidum* in gellan–alginate microparticles. *Biotechnology and Bioengineering*, *98*, 411–419.

Chen, G., Yao, S. J., Guan, Y. X., & Lin, D. Q. (2005). Preparation and characterization of NaCS-CMC/PDMDAAC capsules. *Colloids and Surfaces B: Biointerfaces*, *45*, 136–143.

Choo-Smith, L. P., Maquelin, K., Vreeswijk, T. V., Bruining, H. A., Puppels, G. J., Ngo, T. N. A., et al. (2001). Investigating microbial (micro) colony heterogeneity by vibrational spectroscopy. *Applied and Environmental Microbiology*, *67*, 1461–1469.

Collins, J. W., La Ragione, R. M., Woodward, M. J., & Searle, L. E. J. (2009). Application of prebiotics and probiotics in livestock. In D. Charalampopoulos, & R. A. Rastall (Eds.), *Prebiotics and probiotics science and technology* (pp. 1123–1192). Berlin/Heidelberg: Springer Verlag.

De Angelis, M., Siragusa, S., Berloco, M., Caputo, L., Settanni, L., Alfonsi, G., et al. (2006). Selection of potential probiotic lactobacilli from pig feces to be used as additives in pelleted feeding. *Research in Microbiology*, *157*, 792–801.

de Vos, P., Faas, M. M., Spasojevic, M., & Sikkema, J. (2010). Encapsulation for preservation of functionality and targeted delivery of bioactive food components. *International Dairy Journal*, *20*, 292–302.

Ding, W. K., & Shah, N. P. (2007). Acid, bile, and heat tolerance of free and microencapsulated probiotic bacteria. *Food Microbiology and Safety*, *72*, M446–M450.

Ding, W. K., & Shah, N. P. (2009). Effect of homogenization techniques on reducing the size of microcapsules and the survival of probiotic bacteria therein. *Journal of Food Science*, *74*, M231–M236.

Emregül, E., Sungur, S., & Akbulut, U. (1996). Effect of chromium salts on invertase immobilization onto carboxymethyl-cellulose-gelatine carrier system. *Biomaterials*, *17*, 1423–1427.

FAO/WHO. (2002). *Joint FAO/WHO (Food and Agriculture Organization/World Health Organization) working group report on drafting guidelines for the evaluation of probiotics in food*. London/Ontario, Canada: FAO/WHO., pp. 1–11.

Filip, Z., & Hermann, S. (2001). An attempt to differentiate *Pseudomonas spp.* and other soil bacteria by FT-IR spectroscopy. *European Journal of Soil Biology*, *37*, 137–143.

Gaggìa, F., Mattarelli, P., & Biavati, B. (2010). Probiotics and prebiotics in animal feeding for safe food production. *International Journal of Food Microbiology*, *141*, s15–s28.

Goodacre, R., Timmins, E. M., Rooney, P. J., Rowland, J. J., & Kell, D. B. (1996). Rapid identification of *Streptococcus* and *Enterococcus* species using diffuse reflectance-absorbance Fourier transform infrared spectroscopy and artificial neural networks. *FEMS Microbiology Letters*, *140*, 233–239.

Gouin, S. (2004). Microencapsulation: Industrial appraisal of existing technologies and trends. *Trends in Food Science and Technology*, *15*, 330–347.

Hu, G., Huang, S., Cao, S., & Ma, Z. (2009). Effect of enrichment with hemicellulose from rice bran on chemical and functional properties of bread. *Food Chemistry*, *115*, 839–842.

Idouraine, A., Khan, M. J., Kohlhepp, E. A., & Weber, C. W. (1996). In vitro mineral binding capacity of three fiber sources for Ca, Mg, Cu and Zn by two different methods. *International Journal of Food Sciences and Nutrition*, *47*, 285–293.

Kaihara, S., Suzuki, Y., & Fujimoto, K. (2011). In situ synthesis of polysaccharide nanoparticles via polyion complex of carboxymethyl cellulose and chitosan. *Colloids and Surfaces B: Biointerfaces*, *85*, 343–348.

Kamel, S., Ali, N., Jahangir, K., Shah, S. M., & El-Gendy, A. A. (2008). Pharmaceutical significance of cellulose: A review. *eXPRESS Polymer Letters*, *2*, 758–778.

Kansiz, M., Heraud, P., Wood, B., Burden, F., Beardall, J., & McNaughton, D. (1999). Fourier Transform Infrared microspectroscopy and chemometrics as a tool for the discrimination of cyanobacterial strains. *Phytochemistry*, *52*, 407–417.

Kummerle, M., Scherer, S., & Seiler, H. (1998). Rapid and reliable identification of food-borne yeasts by Fourier-transform infrared spectroscopy. *Applied and Environmental Microbiology*, *64*, 2207–2214.

Kuo, C. K., & Ma, P. X. (2001). Ionically crosslinked alginate hydrogels as scaffolds for tissue engineering: Part 1. Structure, gelation rate and mechanical properties. *Biomaterials*, *22*, 511–521.

Mandal, S., Puniya, A. K., & Singh, K. (2006). Effect of alginate concentrations on survival of microencapsulated *Lactobacillus casei* NCDC-298. *International Dairy Journal*, *16*, 1190–1195.

Moebus, K., Siepmann, J., & Bodmeier, R. (2009). Alginate–poloxamer microparticles for controlled drug delivery to mucosal tissue. *European Journal of Pharmaceutics and Biopharmaceutics*, *72*, 42–53.

Montanher, S. F., Oliveira, E. A., & Rollemberg, M. C. (2005). Removal of metal ions from aqueous solutions by sorption onto rice bran. *Journal of Hazardous Materials*, *B117*, 207–211.

Nakphaichit, M., Thanomwongwattana, S., Phraephaisarn, C., Sakamoto, N., Keawsompong, S., Nakayama, J., et al. (2011). The effect of including *Lactobacillus reuteri* KUB-AC5 during post-hatch feeding on the growth and ileum microbiota of broiler chickens. *Poultry Science*, *90*, 2753–2765.

Nitisinprasert, S., Nilphai, V., Bunyun, P., Sukyai, P., Doi, K., & Sonomoto, K. (2000). Screening and identification of effective thermotolerant lactic acid bacteria producing antimicrobial activity against *Escherichia coli* and *Salmonella* sp. resistant to antibiotics. *Kasetsart Journal (Natural Science)*, *34*, 387–400.

Priya, A. J., Vijayalakshmi, S. P., & Raichur, A. M. (2011). Enhanced survival of probiotic *Lactobacillus acidophilus* by encapsulation with nanostructured polyelectrolyte layers through layer-by-layer approach. *Journal of Agricultural and Food Chemistry*, *59*, 11838–11845.

Sabiki, L., Babu, R., Thompkinson, D. K., & Kapila, S. (2010). Resistance of microencapsulated *Lactobacillus acidophilus* LA1 to processing treatments and simulated gut conditions. *Food and Bioprocess Technology*, *3*, 586–593.

Truelstrup Hansen, L., Allan-Wojtas, P. M., Jin, Y. L., & Paulson, A. T. (2002). Survival of Ca-alginate microencapsulated *Bifidobacterium* spp. in milk and simulated gastrointestinal conditions. *Food Microbiology*, *19*, 35–45.

Vale, J. M., Justice, R. S., Schaefer, D. W., & Mark, J. E. (2007). Calcium alginate barrier films modified by montmorillonite clay. *Journal of Macromolecular Science, Part B*, *44*, 821–831.

Yun, S. E., & Hong, S. T. (2007). Isolation and investigation of emulsifying properties of surface-active substances from rice bran. *Food Hydrocolloids*, *21*, 838–843.